



1 **The underappreciated impact of emission source profiles on the simulation of**
2 **PM_{2.5} components: New evidence from sensitivity analysis**

3 Zhongwei Luo^{a,b,1}, Yan Han^{a,b,c,1}, Kun Hua^{a,b}, Yufen Zhang^{a,b*}, Jianhui Wu^{a,b}, Xiaohui
4 Bi^{a,b}, Qili Dai^{a,b}, Baoshuang Liu^{a,b}, Yang Chen^c, Xin Long^c, Yinchang Feng^{a,b*}

5 ^aState Environmental Protection Key Laboratory of Urban Ambient Air Particulate
6 Matter Pollution Prevention and Control & Tianjin Key Laboratory of Urban
7 Transport Emission Research, College of Environmental Science and Engineering,
8 Nankai University, Tianjin 300350, China.

9 ^bCMA-NKU Cooperative Laboratory for Atmospheric Environment-Health Research,
10 Tianjin 300350, China.

11 ^cResearch Center for Atmospheric Environment, Chongqing Institute of Green and
12 Intelligent Technology, Chinese Academy of Sciences, Chongqing 400714, China.

13

14

15 *Corresponding authors:

16 Y. F. Zhang (zhafox@nankai.edu.cn). And Y. C. Feng (fengyc@nankai.edu.cn).

17

18 ¹Z. W. Luo and Y. Han equally contribute to this work



19 **Abstract**

20 The chemical transport model (CTM) is an essential tool for air quality prediction
21 and management, widely used in air pollution control and health risk assessment.
22 However, the current models do not perform very well in simulating PM_{2.5} components.
23 Studies suggested that the uncertainties of model chemical mechanism, source emission
24 inventory and meteorological field can cause inaccurate simulation results. Still, the
25 emission source profile of PM_{2.5} has not been fully taken into account in current
26 numerical simulation. This study aims to answer (1) Whether the variation of source
27 profile adopted in chemical transport models (CTMs) has an impact on the simulation
28 of PM_{2.5} chemical components? (2) How much does it impact? (3) How does the impact
29 work? Based on the characteristics and variation rules of chemical components in
30 typical PM_{2.5} sources, different simulation scenarios were designed and the sensitivity
31 of components simulation results to PM_{2.5} sources profile was explored. Our findings
32 showed that the influence of source profile changes on simulated PM_{2.5} concentration
33 was insignificant, but its impact on PM_{2.5} components could not be ignored. The
34 variations of simulated components ranged from 8% to 167% under selected different
35 source profiles, and simulation results of some components were sensitive to the
36 adopted PM_{2.5} source profile in CTMs. These influences are connected to the chemical
37 mechanisms of the model since the variation of species allocations in emission sources
38 directly affected the thermodynamic equilibrium system. We also found that the
39 perturbation of the PM_{2.5} source profile caused the variation of simulated gaseous
40 pollutants, which indirectly indicated that the perturbation of the source profile affected
41 the simulation of secondary PM_{2.5} components. Given the vital role of air quality
42 simulation in environment management and health risk assessment, the
43 representativeness and timeliness of source profile should be considered.

44 **Keywords**

45 PM_{2.5}; source profile; component; numerical simulation; chemical transport model



46 **1. Introduction**

47 Ambient fine particulate matter (PM_{2.5}) pollution in some key regions of China
48 has attracted much attention (Liang et al., 2020; Huang et al., 2021). The chemical
49 components of PM_{2.5}, including elements (Al, Si, Fe, Mn, Ti, Cu, Zn, Pb, etc.), water-
50 soluble ions (SO₄²⁻, NO₃⁻, Cl⁻, F⁻, NH₄⁺, Na⁺, K⁺, Mg²⁺, Ca²⁺, etc.), and carbon-
51 containing components (Organic Carbon, OC; Elemental Carbon, EC) (Yang et al.,
52 2011; Li et al., 2013), have different physical and chemical properties, such as reactivity,
53 thermal stability, particle size distribution, residence time, optical properties, health
54 hazards, etc (Seinfeld and Pandis, 2006; Tang et al., 2006). According to long-term
55 monitoring results, in most regions of China, SO₄²⁻, NO₃⁻, NH₄⁺ and OC are the most
56 important species in ambient PM_{2.5} (Li et al., 2017a; Li et al., 2021), which has a certain
57 adverse impact on human health (Shi et al., 2018) and ecosystem (Han et al., 2019;
58 Zhou et al., 2018), such as acid rain in southwest China (Han et al., 2019), food security
59 (Zhou et al., 2018), etc.

60 The chemical transport models (CTMs) play an important role in policy making
61 for regulatory purposes. Based on the scientific understanding of atmospheric physical
62 and chemical processes, CTMs are built to simulate the transport, reaction and removal
63 of pollutants on a certain scale in horizontal and vertical directions. With the
64 development of CTMs, the simulation accuracy of PM_{2.5} concentration has been
65 significantly improved. Higher requirements have been put forward for the precise
66 simulation of PM_{2.5} components so as to provide support for the use of CTMs in human
67 health risk assessment, climate effects, pollution sources apportionment, and so on
68 (Peterson et al., 2020; Lv et al., 2021). However, the current models perform not very
69 well in simulating some components (for example, PM_{2.5}-bound sulfate, nitrate,
70 ammonium, trace elements, etc.) (Zheng et al., 2015; Fu et al., 2016; Ying et al., 2018;
71 Cao et al., 2021). In the current literature, the correlation coefficient (R) and normalized
72 mean bias (NMB) are highly variable and inconsistent between the simulated and the
73 observed values (listed in Table S1). This is mainly attributable to the uncertainties of



74 model chemical mechanism, source emission inventory and meteorological field
75 simulation.

76 The chemical mechanisms involved in CTMs are derived from parameterized
77 assumptions based on laboratory simulation and field observations. The actual
78 atmospheric chemical processes are very complex, and some reaction mechanisms are
79 still limitedly understood. In addition, the integration of chemical reactions and
80 simplified treatment methods in the model cannot fully reflect the correlation among
81 atmospheric pollutants. For example, in some model mechanisms, other important
82 sulfate and nitrate formation pathways were added through new heterogeneous
83 chemistry, including the chemical reaction between SO_2 and aerosol, $\text{NO}_2/\text{NO}_3/\text{N}_2\text{O}_3$
84 and aerosol (Zheng et al., 2015), nitrous acid oxidized SO_2 to produce sulfate (Zheng
85 et al., 2020), dust particles promoted the oxidation of SO_2 (Yu et al., 2020), modified
86 the uptake coefficients for heterogeneous oxidation of SO_2 to sulfate (Zhang et al.,
87 2019), updated the heterogeneous N_2O_5 parameterization (Foley et al., 2010). Even
88 though the aforementioned processes can significantly improve the simulation of SO_4^{2-}
89 and NO_3^- , there is still a gap between the modeled and the actual atmospheric chemical
90 processes.

91 The uncertainty of source emission inventory also significantly affects the
92 simulation results of $\text{PM}_{2.5}$ components (Shi et al., 2017; Sha et al., 2019). Due to
93 incomplete information or insufficient representativeness, pollutant emissions are
94 sometimes overestimated or underestimated, and the method for temporal and spatial
95 allocation also needs to be improved.

96 The uncertainty of meteorological field simulation is another crucial reason for the
97 simulation deviation, especially on heavy pollution days, the variation trends of $\text{PM}_{2.5}$
98 chemical components were not well-captured (Ying et al., 2018; Qi et al., 2019; Wang
99 et al., 2022). Precipitation is the key meteorological factor determining wet removal of
100 pollutants; boundary layer height and wind speed are the main factors affecting
101 convection and transport of pollutants; solar radiation, temperature and relative
102 humidity are the key factors affecting the formation of secondary particles (Huang et



103 al., 2019; Chen et al., 2020). Some literature reported that deviation from precipitation
104 and wind field simulation might lead to underestimation of SO_4^{2-} , NO_3^- and NH_4^+
105 (Cheng et al., 2015; Zhang et al., 2017). Devaluation of liquid water path and cloud
106 cover cause a decrease of sulfate formation in cloud, and ultimately results in
107 significantly underestimated components in simulation values (Sha et al., 2019; Foley
108 et al., 2010). Underestimation of temperature and relative humidity may also cause
109 adverse effects of temperature- and/or relative humidity-dependence chemical reaction
110 in the simulation (Sha et al., 2019).

111 In particular, the emission source profile of $\text{PM}_{2.5}$ (Hereinafter referred to as
112 "source profile") has not been fully taken into account in the current numerical
113 simulation by CTMs. In the reported literature, $\text{PM}_{2.5}$ species allocation coefficients of
114 emission sources are commonly treated in the following ways: (1) allocated $\text{PM}_{2.5}$
115 components of source emissions by referring to source profile data in published
116 literature or database like the US SPECIATE (Fu et al., 2013; Wang et al., 2014; Ying
117 et al., 2018); (2) chemical profiles come from local measurement (Fu et al., 2013; Appel
118 et al., 2013). However, with the development of production technology and the
119 innovation of pollution treatment technology in recent years, some source profiles have
120 changed dramatically (Bi et al., 2019), such as SO_4^{2-} from coal burning, SO_4^{2-} content
121 in $\text{PM}_{2.5}$ is generally low in coal-fired power plant without desulfurizing facilities, while
122 existing coal-fired power plants using limestone/gypsum wet desulphurization, the
123 contents of SO_4^{2-} in $\text{PM}_{2.5}$ are significantly higher than that without desulfurization
124 facilities (Zhang et al., 2020). The timeliness of $\text{PM}_{2.5}$ species allocation coefficients in
125 current CTMs also needs to be considered.

126 This paper attempts to answer the following questions: (1) Whether the variation
127 of the source profile adopted in the air quality model has an impact on the simulated
128 results of $\text{PM}_{2.5}$ chemical components? (2) How much does it impact? (3) How does
129 the impact work? Aiming at these problems above, chemical composition and its
130 variation law for typical $\text{PM}_{2.5}$ emission sources are summarized, on this basis,
131 sensitivity tests are designed to identify whether $\text{PM}_{2.5}$ source profiles and species

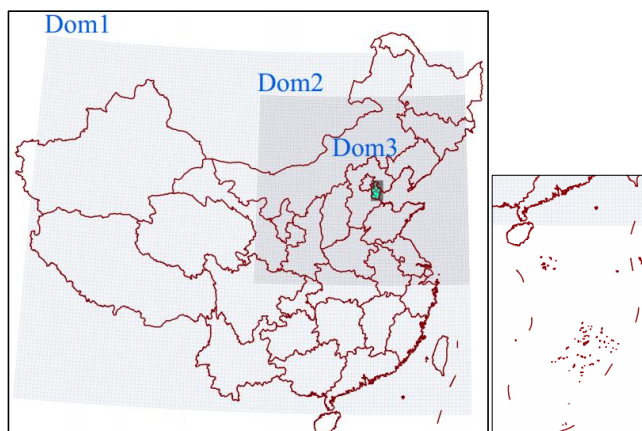


132 allocation in the model are important parameters that affect the simulation results of
133 chemical components in $PM_{2.5}$. The aim of this study is to provide support for the
134 effective utilization of source profiles in the CTMs and improvement of the simulation
135 schemes.

136 **2. Model and Data**

137 **2.1 Model configuration**

138 Weather Research and Forecasting model (WRF-3.7.1), the widely used
139 Community Multiscale Air Quality model (CMAQv5.0.2), and Multi-resolution
140 Emission Inventory for China (MEICv1.3) have been used in this study. MEIC provided
141 the emission inventory which is developed by Tsinghua University, mainly tracked
142 anthropogenic emissions in China including coal-fired power plants, industry, vehicles,
143 residents and agriculture (http://meicmodel.org/?page_id=135) (Li et al., 2017b; Zheng
144 et al., 2018). The WRF model was used to generate meteorological inputs for the
145 CMAQ model. Three nested modeling domains consisting of 36 km×36 km (Dom1),
146 12 km×12km (Dom2), and 4 km×4km (Dom3) horizontal grid sizes were set, as shown
147 in Fig. 1. The initial and boundary conditions for WRF were based on the North
148 American Regional Reanalysis data archived at National Center for Atmospheric
149 Research (NCAR). In addition, surface and upper air observations obtained from
150 NCAR were used to further refine the analysis data. The major configurations we used
151 in CMAQ were illuminated as follows: Gas-phase chemistry was based on the CB05
152 mechanism and the aerosol dynamics/chemistry was based on the aero6 module
153 (cb05tucl_ae6_aq). The detailed model configurations were shown in Table S2.



154
155

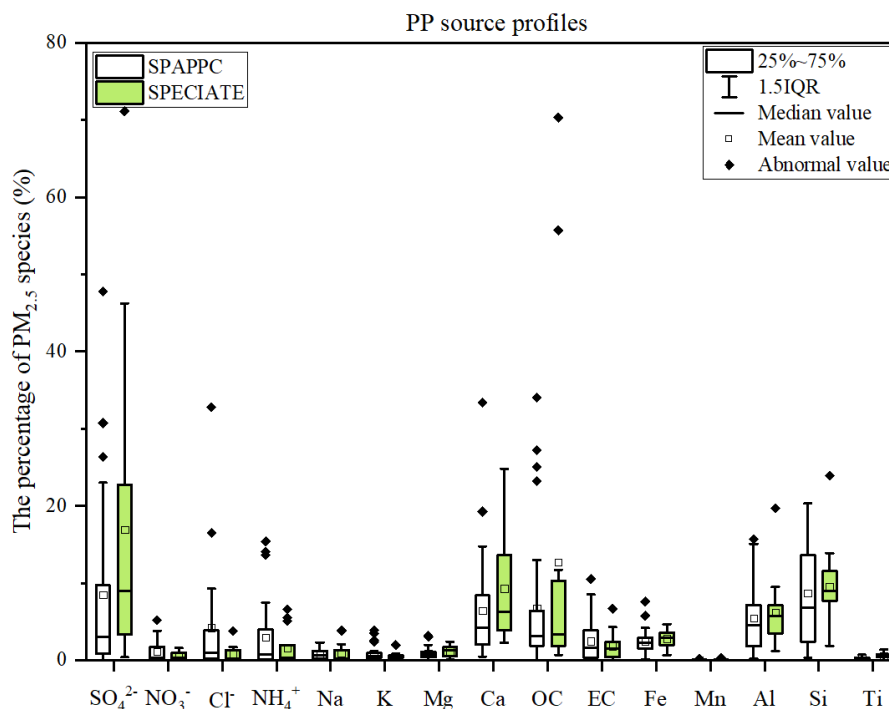
Fig.1 Modeling domains of the CMAQ model

156 2.2 Selection and comparison of PM_{2.5} source profile

157 The PM_{2.5} emission source profiles from database of Source Profiles of Air
158 Pollution (SPAP) (<http://www.nkspap.com:9091/>), U.S. Environmental Protection
159 Agency's (EPA) SPECIATE database ([https://www.epa.gov/air-emissions-
160 modeling/speciate](https://www.epa.gov/air-emissions-modeling/speciate)) as well as from published literature were selected, respectively. The
161 SPAP was developed by the State Environment Protection Key Laboratory of Urban
162 Particulate Air Pollution Prevention, Nankai University, China. This database contains
163 more than 3000 size-resolved source profiles of stationary combustion sources,
164 industrial processes, vehicle exhaust, biomass burning, dust and cooking emissions and
165 other sources, collected from more than 40 cities in China since 2001. In addition to
166 inorganic elements, water-soluble ions, OC, EC and other conventional components,
167 some source profiles also encompass a series of tracer information, such as organic
168 markers, isotopes, single particle mass spectrometry, VOCs and other gaseous
169 precursors. Based on species in the aerosol chemical mechanism (AERO6) (Appel et
170 al., 2013; Chapel Hill, 2012), we selected 15 components in PM_{2.5} source profiles
171 including Al, Ca, Cl, EC, Fe, K, Mg, Mn, Na, OC, Si, Ti, NH₄⁺, NO₃⁻ and SO₄²⁻, the
172 remaining components are classified as "other". Emission sources are divided into four
173 main categories referred to the classification in MEIC: coal combustion by power plants
174 (PP), industrial processes (IN), residential emission (RE) and transportation sector (TR).
175 Coal-fired power plants remain the main coal consumers in China, which

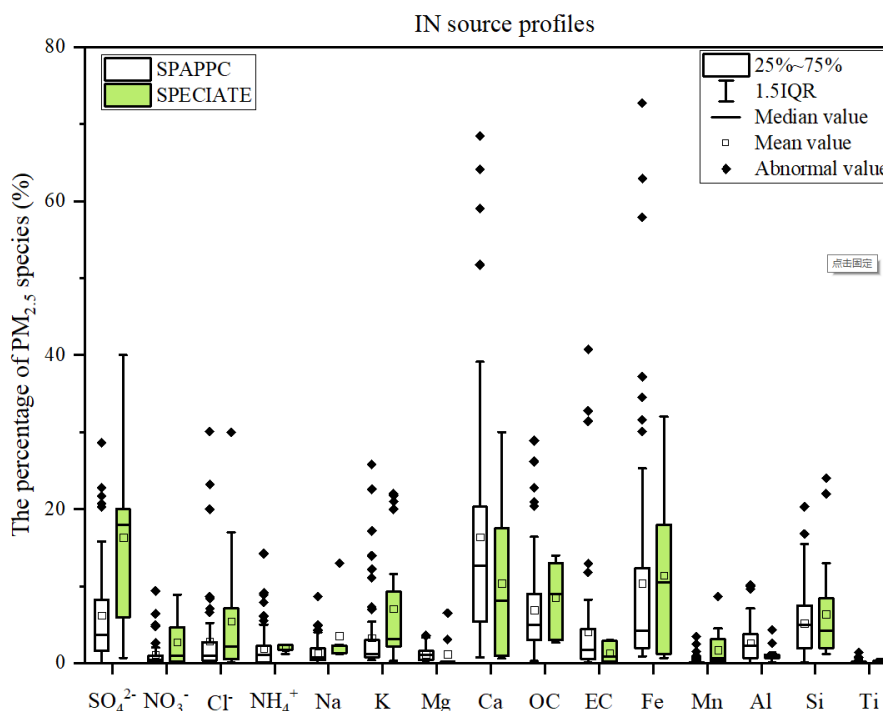


176 accounted for 50.2% of total coal consumption in 2019 (NBS, 2021) and gained much
177 more attention (Wu et al., 2022), especially with the wide implementation of the
178 strictest ultralow emission standards, PM_{2.5} emission characteristics have changed
179 accordingly (Wu et al., 2020). There are obvious differences in PM_{2.5} source profiles
180 between SPAPPC (SPAP database and published source profiles in China) and
181 SPECIATE (SPECIATE database), detailed information is shown in Table S3. The
182 percentages of species in PP source profiles are plotted in Fig. 2. The main components
183 in SPAPPC are sorted by Si, SO₄²⁻, OC, Ca with average values of 8.7±6.8%, 8.5±11.5%,
184 6.8±9.1% and 6.5±6.9%, respectively; The SPECIATE are enriched in SO₄²⁻
185 (16.9%±20.0%), OC (12.7±21.8%), Si (9.6±5.0%) and Ca (9.3±7.3%), higher than
186 SPAPPC. Coal properties, burning conditions, pollution control measures and sampling
187 methods are the main reasons for those great percentage fluctuations. Different
188 treatment processes of flue gases, e.g. wet/dry limestone, ammonia and double-alkali
189 flue gas desulfurization, will affect the percentages of components in source profiles
190 (Zhang et al., 2020). It has been reported that the percentage of Ca, Mg, SO₄²⁻ and Cl⁻
191 in PP profiles increased after the limestone-gypsum method was used in coal-fired
192 power plants (Bi et al., 2019). Besides that, the percentage of Cl⁻ in SPAPPC is
193 obviously higher than that in SPECIATE, which might attribute to the generally higher
194 Cl⁻ content in raw coal in China (Guo et al., 2004).



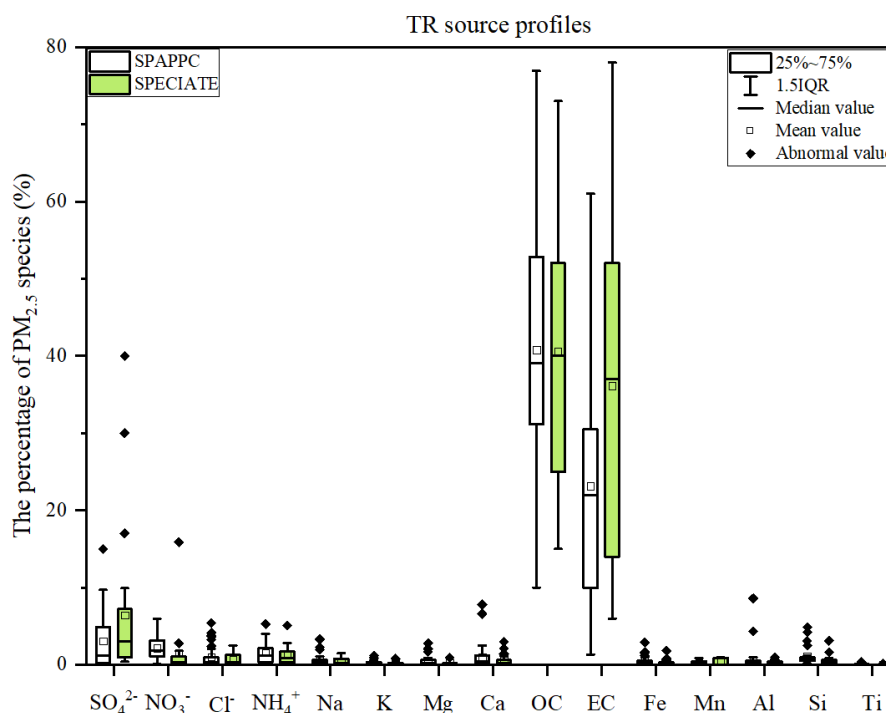
195
 196 Fig. 2 Chemical profiles for PM_{2.5} emitted from coal-fired power plant (PP). Data obtained from
 197 SPAPPC (SPAP database and published source profiles in China) and SPECIATE (U.S. EPA
 198 SPECIATE database)

199 Industrial emissions are one of the major sources of PM_{2.5} (Hopke et al., 2020),
 200 the percentages of Ca, Fe, OC and SO₄²⁻ are relatively high both in SPAPPC and
 201 SPECIATE of industrial processes, but the shares in different source profile database
 202 varied (Detailed information were shown in Table S4~S7). In SPAPPC, these four
 203 components account for 16.4±14.9%, 10.4±14.4%, 6.9±6.1%, 6.2±6.4%, the
 204 proportions in SPECIATE are 10.4±9.8%, 11.4±10.6%, 8.5±4.9%, 16.3±13.3%,
 205 respectively (Fig. 3). Large variations of components and their percentages in industrial
 206 processes are attributed to the manufacturing processes, raw material, pollution control
 207 measures and so on (Ji et al., 2017; Bi et al., 2019; Gao et al., 2022). For example, Ca,
 208 Al, OC and SO₄²⁻ are found to have the highest percentage in cement sources (Guo et
 209 al., 2021); Fe, Si and SO₄²⁻ are the most abundant species in steel industry emission
 210 (Guo et al., 2017).



211
 212 Fig. 3 Chemical profiles for PM_{2.5} emitted from industry processes (IN). Data obtained from
 213 SPAPPC (SPAP database and published source profiles in China) and SPECIATE (U.S. EPA
 214 SPECIATE database)

215 Traffic contributed a large fraction of PM_{2.5} in many locations (Hopke et al., 2022).
 216 It is well-known that the transportation sector makes a dominant contribution of OC
 217 and EC. The main components of PM_{2.5} emitted from traffic sources are OC, EC and
 218 SO₄²⁻ both in SPAPPC and SPECIATE, but still vary in wide range (Detailed
 219 information was given in Table S8–S10). In SPAPPC, the percentages of OC, EC and
 220 SO₄²⁻ are 40.8±15.0%, 23.1±13.8%, 3.1±3.7%, and in SPECIATE, the percentages are
 221 40.6±16.4%, 36.1±21.5%, 6.4±9.9%, respectively (Fig. 4). These significant
 222 differences mainly attribute to the vehicle type, fuel quality, mixing ratio between oil
 223 and gas and the combustion phase in vehicle engine and so on (Xia et al., 2017).

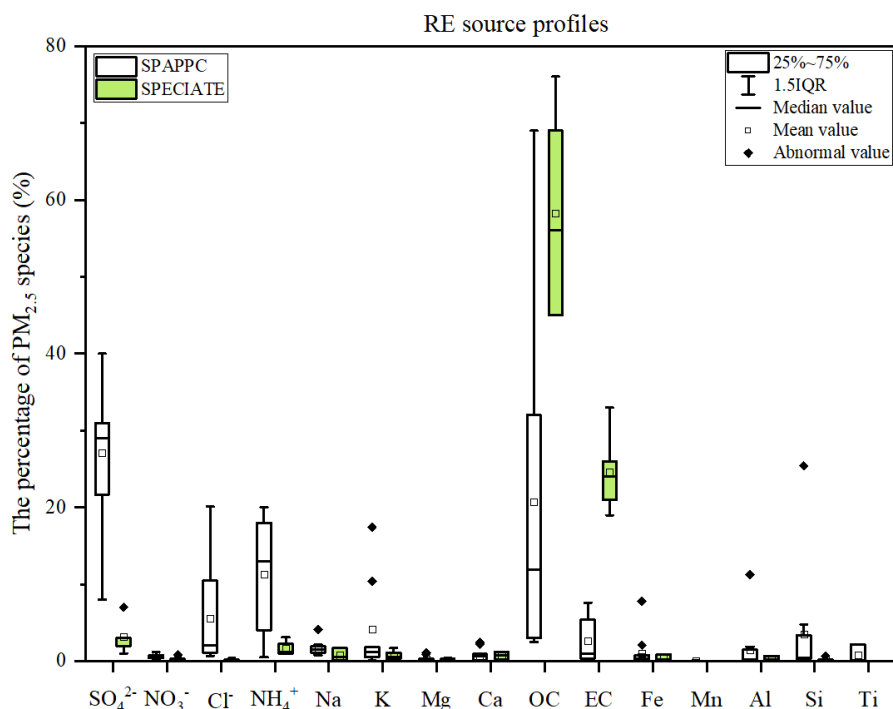


224
225 Fig. 4 Chemical profiles for PM_{2.5} emitted from transportation sector (TR). Data obtained from
226 SPAPPC (SPAP database and published source profiles in China) and SPECIATE (U.S. EPA
227 SPECIATE database)

228 Residential coal combustion, as the leading source of global PM_{2.5} emission
229 (Weagle et al., 2018), has a much higher emission factor than coal-fired power plant
230 (Wu et al., 2022). The fraction of components varied greatly in the profiles measured
231 from SPAPPC and SPECIATE (Detailed information was given in Table S11), SO₄²⁻,
232 OC, NH₄⁺ and EC make the main contribution to PM_{2.5} emitted from residential coal
233 combustion. In SPAPPC, the average percentages of SO₄²⁻, OC, NH₄⁺, EC are
234 27.1±10.1%, 20.7±20.6%, 11.3±7.7%, 2.6±2.8%, respectively. In SPECIATE, the
235 average percentages are OC (58.2±14.0%), EC (24.6±5.4%), SO₄²⁻ (3.2±2.3%) and
236 NH₄⁺ (1.6±1.0%) (Fig. 5). Total percentages of OC and EC in SPECIATE are over 80%,
237 obviously higher than that in SPAPPC, while a higher percentage of SO₄²⁻, Cl⁻, K and
238 Si are observed in SPAPPC. The coal type and properties, burning condition are the
239 main factors affecting the percentages of PM_{2.5} components, like the chunk coal burning
240 has relatively higher percentages of OC, EC, SO₄²⁻, NO₃⁻ and NH₄⁺ than honeycomb



241 briquette (Wu et al., 2021; Song et al., 2021).



242
243 Fig. 5 Chemical profiles for PM_{2.5} emitted from residential coal combustion (RE). Data obtained
244 from SPAPPC (SPAP database and published source profiles in China) and SPECIATE (U.S. EPA
245 SPECIATE database)

246 Briefly, many factors can affect PM_{2.5} source profiles, and with the innovation of
247 manufacturing technique and pollution control technology, changes in fuel and raw and
248 auxiliary materials, the main chemical components and their percentages would change
249 dramatically. To explore whether the variations of source profile would be one of the
250 important factors affecting the simulation results of PM_{2.5} species in CTMs, we
251 designed a series of simulation tests as follows.

252 3 Whether the variation of source profile adopted in CTMs has an impact on the 253 simulation of chemical components in PM_{2.5}?

254 In this part, we separately selected source profiles from SPAPPC and SPECIATE
255 databases and applied them in emission inventory for simulating PM_{2.5} and its
256 components with other modeling conditions unchanged, corresponding to case



257 CMAQ_SPA and CMAQ_SPE. The detailed information on source profiles is shown
258 in Figure S1. To determine the similarity between the two groups of source profiles,
259 Coefficient divergence (CD) is calculated using the following formula
260 (Wongphatarakul et al., 1998):

261
$$CD_{jk} = \sqrt{\frac{1}{p} \sum_{i=1}^p \left(\frac{x_{ij} - x_{ik}}{x_{ij} + x_{ik}} \right)^2} \dots\dots\dots (1)$$

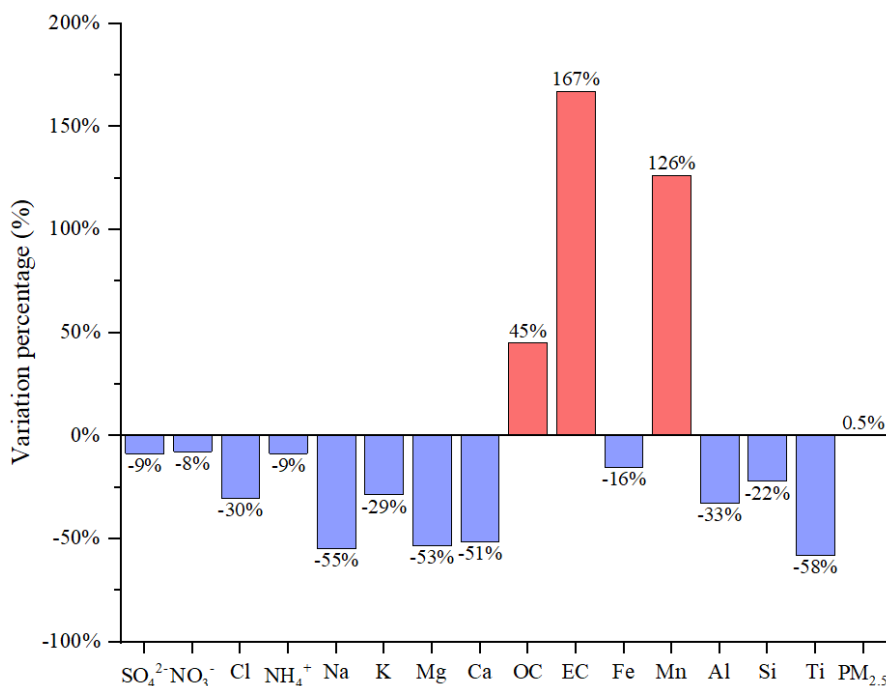
262 Where CD_{jk} is the coefficient of divergence of source profile j and k , p was the
263 number of chemical components in source profile, x_{ij} is the weight percentage for
264 chemical component i in source profile j , x_{ik} is the weight percentage for i in source
265 profile k (%). The CD value is in the range of 0 to 1, if the two source profiles are
266 similar, the value of CD is close to 0; if the two are very different, the value was close
267 to 1.

268 By comparing the selected SPAPPC source profiles with the selected SPECIATE
269 source profiles, the coefficient divergences for the four main source categories were
270 $CD_{PP}(0.67) > CD_{RE}(0.62) > CD_{TR}(0.60) > CD_{IN}(0.60)$, which meant the selected source
271 profiles in the two simulation cases were quite different. The simulated concentration
272 of $PM_{2.5}$ and its components (For this part and each test case in next section) at 10
273 ambient air quality monitoring stations (Table S12) were extracted from CMAQ outputs
274 of the innermost simulation domain. We selected one air quality monitoring station to
275 study the influence of $PM_{2.5}$ source profile on numerical simulation of $PM_{2.5}$ -bound
276 components and to explore the relevant laws in the atmosphere, then used the left 9 sites
277 to further illustrate the conclusions suggested.

278 The simulation results for $PM_{2.5}$ species under CMAQ_SPA and CMAQ_SPE
279 cases also showed big differences (as shown in Fig. 6 and Table S13), in which the
280 largest difference in simulated concentration was EC with CAMQ_SPE giving higher
281 by 167% than CMAQ_SPA; For OC and Mn, higher values were also given by
282 CMAQ_SPE than by CMAQ_SPA (45% and 126% on average, respectively); For the
283 remaining components, the simulated concentration by CMAQ_SPE was lower than
284 CMAQ_SPA with Ti (58%), Na (55%), Mg (53%), Ca (51%), Al (33%), Cl (30%), K



285 (29%), Si (22%), Fe (16%), NH_4^+ (9%), SO_4^{2-} (9%), NO_3^- (8%), separately. While the
286 simulated $\text{PM}_{2.5}$ concentrations under the two cases were quite close. The influence of
287 source profile variation on the simulated $\text{PM}_{2.5}$ concentration was not significant, but
288 the influence on the simulation of chemical components in $\text{PM}_{2.5}$ could not be ignored.



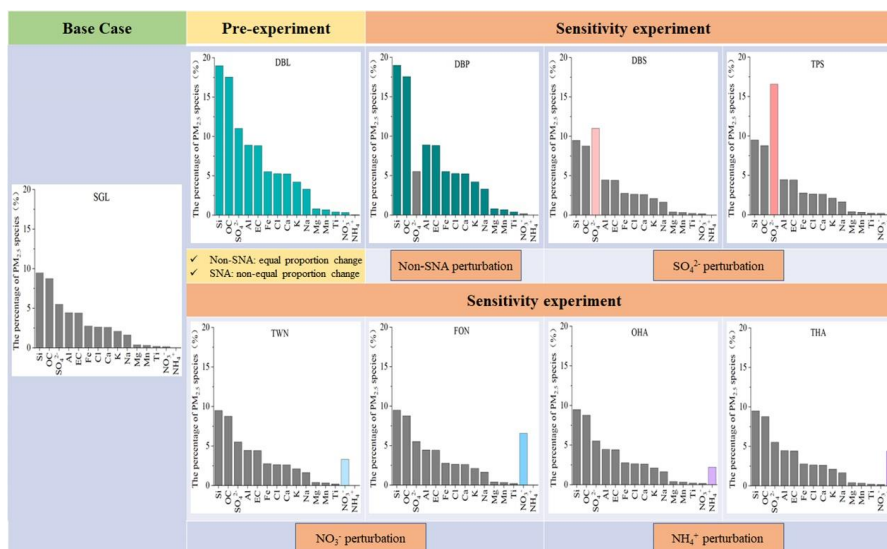
289
290 Fig. 6 The percentage difference of simulated concentration ($\text{PM}_{2.5}$ and its components) between
291 CMAQ_SPE and CAMQ_SPA (relative to CAMQ_SPA); $\text{PM}_{2.5}$ source profiles from SPAPPC and
292 SPECIATE database were applied in emission inventory for simulating $\text{PM}_{2.5}$ and its components,
293 corresponding to case CMAQ_SPA and CMAQ_SPE, respectively.

294 **4 How much did the variation of source profile adopted in CTMs impact on the** 295 **simulation of chemical components in $\text{PM}_{2.5}$?**

296 In order to quantitatively characterize how much the source profiles affect the
297 simulation results of $\text{PM}_{2.5}$ and its components, we selected the chemical composition
298 of code 000002.5 (Variety of different categories, used for the overall average
299 composite profiles (Hsu et al., 2019)) in the US EPA Speciate_5.0_0 database as species



300 allocation of PM_{2.5} components. The corresponding percentages of EC, OC, Mn, Fe, Ti,
 301 Al, Si, Ca, Mg, K, Na, Cl, NH₄⁺, NO₃⁻ and SO₄²⁻ in PM_{2.5} were shown in Fig. 7 (SGL,
 302 base case simulation).



303
 304 Fig. 7 The general roadmap of sensitivity tests
 305 (The histogram in each case were the speciation profile in CTMs)

306 Table 1 The content of sensitivity experiment cases

Cases	Description
Pre-experiment (DBL)	The percentage of all the listed components in the source profile of base case (SGL) were doubled, and the proportion of unlisted components (Other) decreased to 9%.
Case S1 (DBP): add perturbation to Non-SNA	The percentages of non-SNA were doubled and SNA(SO ₄ ²⁻ , NO ₃ ⁻ , NH ₄ ⁺) species stayed the same with that in SGL (the cumulative percentage of listed species was 85.3%), the proportion of unlisted components decreased to 14.7%.
Case S2 (DBS and TPS): add perturbation to SO ₄ ²⁻	The percentage of SO ₄ ²⁻ was doubled (11%, DBS, represented Double Sulfate), tripled (16.5%, TPS, represented Triple Sulfate) and the other listed 14 species stayed the same with that in SGL (the cumulative percentage of listed species was 51% and 57%, respectively), the proportion of unlisted components decreased to 49% and 43%.
Case S3 (TWN and FON): add perturbation to NO ₃ ⁻	The NO ₃ ⁻ content was raised up to 20 times (3.3%, TWN) and 40 times (6.6%, FON) of that in SGL (0.16%), the other 14 species stayed the same with SGL (the cumulative



	percentage of listed species was 48.6% and 51.9%, respectively), the proportion of unlisted components decreased to 51.4% and 48.1%.
Case S4 (OHA and THA): add perturbation to NH_4^+	The NH_4^+ content was raised up to 100 times (2.2%, OHA), 200 times (4.4%, THA) of that in SGL (0.02%), the other 14 species stayed the same with SGL (the cumulative percentage of listed species was 47.7% and 49.9%, respectively), the proportion of unlisted components decreased to 52.3% and 50.1%.

Note: The source profiles in all cases listed in the table were calculated based on the base case SGL. In the design of simulation cases, the reason why the disturbance amplitude of NH_4^+ and NO_3^- were significantly higher than that of other components such as SO_4^{2-} and Non-SNA, was because the percentages of NH_4^+ and NO_3^- in the base source profile (SGL, based on the chemical composition of code 000002.5 in the EPA Speciate_5.0_0 database) were very low, while the percentage of NH_4^+ and NO_3^- in SPAPPC exhibited in section 2.2 were orders of magnitude higher than those in SGL.

307 Given the large number and complex chemical composition of $\text{PM}_{2.5}$, it is
308 advisable to classify it reasonably before designing sensitivity experiments. The pre-
309 experiment was to double the percentage of the listed 15 components mentioned above
310 (SGL) in $\text{PM}_{2.5}$ species allocation for emission sources (DBL case, the cumulative
311 percentage was 91%, the details were shown in Fig. 7 and Table 1). As the percentage
312 of these components increased, the proportion of unlisted components (represented by
313 Other) decreased to 9% in order to meet the requirement that the total percentage of all
314 components is 100%. Then we compared the simulation results before (SGL case) and
315 after perturbation (DBL case) in species allocation of $\text{PM}_{2.5}$ sources.

316 In the case DBL, when the percentage of all the components except “other” were
317 doubled in the source profile, the simulated concentrations of Al, Ca, Cl, EC, Fe, K,
318 Mg, Mn, Na, OC, Si and Ti doubled as well, while the simulated concentration of NO_3^- ,
319 SO_4^{2-} and NH_4^+ only increased at about 3%, 10% and 4%, respectively, although the
320 simulated concentration of $\text{PM}_{2.5}$ was not obviously changed (Detailed simulation
321 results were shown in Table S14). Through this pre-experiment, we found that the
322 results for SNA (SO_4^{2-} , NO_3^- , and NH_4^+) and Non-SNA were obviously different.
323 Therefore, we divided the components in the source profile into two groups (Non-SNA
324 and SNA) and designed a series of sensitivity tests listed in next section to further



325 explore how species allocation of PM_{2.5} in emission sources of CTMs would affect the
 326 simulation results.

327 4.1 Sensitivity tests design

328 Based on the pre-experiment results, sensitivity tests were designed by changing
 329 the percentages of the target components and related components in the base case (SGL):
 330 perturbation on each component of Non-SNA, perturbation on SO₄²⁻, perturbation on
 331 NO₃⁻, and perturbation on NH₄⁺. The general roadmap of sensitivity tests was shown in
 332 Fig. 7, and the illustration of each case was summarized in Table 1. The basic rules must
 333 be followed: a) perturbation on the percentage of each component in source profile fell
 334 within the variation range of its measured value described in section 2.2. b) The sum of
 335 the percentage of listed Non-SNA, SNA and Other components in PM_{2.5} source profile
 336 was 100%.

337 4.2 Evaluation index for simulation result

338 In order to quantify the concentration changes of simulated PM_{2.5} components
 339 caused by the perturbation in source profile, we proposed the sensitivity coefficient (δ)
 340 as evaluation index. The calculation formula is as follows:

$$341 \quad \delta_i = \begin{cases} \frac{\frac{C_{i_case}}{C_{PM_{2.5_case}}} \times 100\% - \frac{C_{i_base}}{C_{PM_{2.5_base}}} \times 100\%}{P_{i_case} - P_{i_base}} & \text{(For DBL and DBP)} \\ \frac{\frac{C_{i_case}}{C_{PM_{2.5_case}}} \times 100\% - \frac{C_{i_base}}{C_{PM_{2.5_base}}} \times 100\%}{P_{j_case} - P_{j_base}} & \text{(For other cases)} \end{cases} \dots\dots\dots (2)$$

342 Wherein, δ_{*i*} is the sensitivity coefficient of component *i*, representing the change
 343 of the simulated value of its content in ambient PM_{2.5} corresponded to 1% perturbation
 344 in the source profiles. C_{*i*_case} is the simulation result of component *i* in different
 345 sensitivity experiment cases, μg/m³; C_{*i*_base} is the simulation result of components *i* in
 346 base case, μg/m³; C_{PM_{2.5}_case} is the simulation result of PM_{2.5} in different sensitivity
 347 experiment cases, μg/m³; C_{PM_{2.5}_base} is the simulation result of PM_{2.5} in base case, μg/m³;
 348 P_{*i*_case} is the percentage of component *i* in different source profile of sensitivity

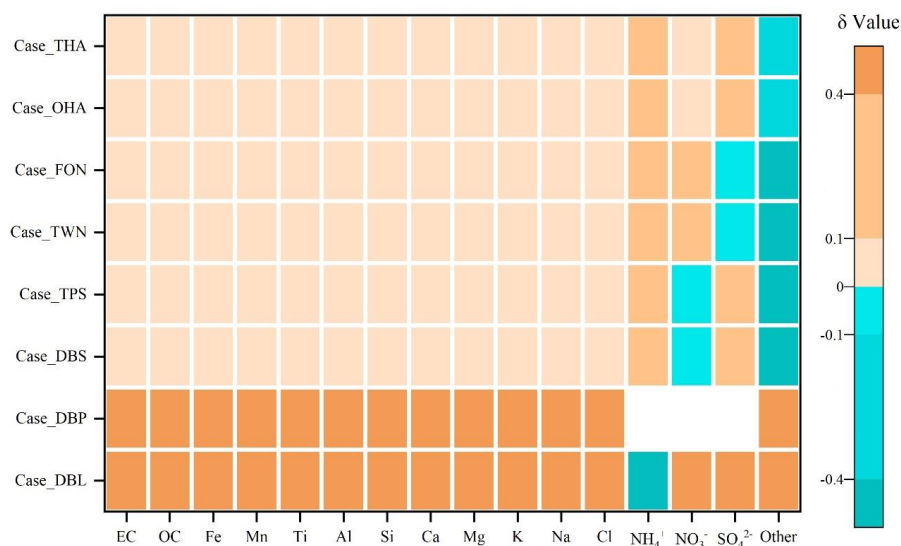


349 experiment cases, %; P_{j_case} is the percentage of perturbed component j in different
350 source profile of sensitivity experiment cases, %; P_{i_base} is the percentage of component
351 i in base case source profile, %; ; P_{j_base} is the percentage of perturbed component j in
352 base case source profile, %.

353 The positive value of δ means the simulated concentration of $PM_{2.5}$ component
354 increases (decreases) with the increase (decrease) of the perturbation to the percentage
355 of components in source profile, while the meaning of negative δ is just the opposite. If
356 the absolute value of δ is less than or equal to 0.1, the simulated result of $PM_{2.5}$ chemical
357 component is considered to be insensitive to the corresponding variation of source
358 profile; If the absolute value of δ falls between 0.1 and 0.4 (included), the simulated
359 results of $PM_{2.5}$ chemical component is considered to be sensitive to the variation of
360 source profile; If the absolute value of δ is larger than 0.4, the simulated results of $PM_{2.5}$
361 chemical component is very sensitive to the variation of source profile. The greater the
362 absolute value of δ is, indicates the variation of source profile adopted in CMAQ has
363 more obvious impact on the simulated results of $PM_{2.5}$ chemical components.

364 **4.3 The response of simulated $PM_{2.5}$ components**

365 Fig.8 listed the sensitivity coefficients of simulated ambient $PM_{2.5}$ components to
366 the perturbation of source profile under each test case. In case DBL (The percentage of
367 all the listed components in the source profile of base case (SGL) was doubled), the
368 sensitivity coefficient (δ) of NH_4^+ was negative, and the absolute value was the highest,
369 indicating that the simulated proportion of NH_4^+ in ambient $PM_{2.5}$ decreased, and it was
370 very sensitive to the variation of source profile. Conversely, the sensitivity coefficient
371 of NO_3^- was close to 1, which illustrated that the simulated proportion of NO_3^- in
372 ambient $PM_{2.5}$ increased proportionally with the change in source profile. The δ of SO_4^{2-}
373 also showed a very sensitive property. The simulated Non-SNA concentrations were
374 doubled when compared to the base case (SGL).



375
376 Fig. 8 The sensitivity coefficients (δ) of simulated components to the perturbation of adopted source
377 profile in different cases. Note: Each small color box in the figure represented the sensitivity level
378 (indicated by the legend on the right) of PM_{2.5} components (the x-coordinate) in different cases (y-
379 coordinate). The blank grids in DBP case indicated no perturbation to SNA in PM_{2.5} source profile
380 under this case.

381 In case DBP, when the percentages of listed Non-SNA in the source profile were
382 doubled, the simulated proportions of Non-SNA (Al, Ca, Cl, EC, Fe, K, Mg, Mn, Na,
383 OC, Si and Ti) in ambient PM_{2.5} synchronous increased, and were very sensitive to the
384 change in the adopted source profile with a sensitivity coefficient (δ) of 0.5.
385 Interestingly, the simulated concentration of SNA in ambient PM_{2.5} also changed
386 although the SNA in source profile did not change, the concentration of NO₃⁻ and SO₄²⁻
387 increased by 2% and 3%, respectively, NH₄⁺ decreased by 10% (Detail simulation
388 results of different cases were shown on Table S15~S21).

389 Under SO₄²⁻ perturbation cases (Case DBS and Case TPS), we found the simulated
390 results of Non-SNA and NO₃⁻ had no obvious variation when compared with the base
391 case. Either in Case DBS or in Case TPS, the δ of Non-SNA and NO₃⁻ were always
392 between -0.1 to 0.1. But when the percentage of SO₄²⁻ was doubled in PM_{2.5}
393 profile (DBS), the simulated concentration of NH₄⁺ and SO₄²⁻ increased by 6% and 8%,
394 respectively. In Case TPS (the percentage of SO₄²⁻ was tripled), the simulated



395 concentration of NH_4^+ and SO_4^{2-} were increased by 11% and 16%, respectively. The δ
396 of NH_4^+ and SO_4^{2-} were 0.12 and 0.36, sensitive toward to positive direction with the
397 increase of SO_4^{2-} in the source profile.

398 In the situation of NO_3^- perturbation (Case TWN and Case FON), the simulated
399 concentrations of Non-SNA hardly change when compared to the base case, while the
400 changing characteristics of SNA concentrations were different. In cases TWN and FON,
401 the simulation concentration of NH_4^+ increased by 2.6% and 5.4% when compared with
402 the base case, the simulated NO_3^- increased by 14% and 30%, the simulated SO_4^{2-}
403 decreased slightly, even could be neglected in some observation sites. The simulated
404 concentrations of Non-SNA and SO_4^{2-} were insensitive to the perturbation of NO_3^- in
405 $\text{PM}_{2.5}$ source profile; NH_4^+ was sensitive, and NO_3^- was very sensitive.

406 When we put perturbation to NH_4^+ in the source profile (Case OHA and Case
407 THA), the simulation results of Non-SNA were almost not changed, the simulated
408 concentration of SO_4^{2-} , NH_4^+ , NO_3^- increased in OHA and THA. The δ of SNA to the
409 variation of NH_4^+ in the source profile were positive and $\delta(\text{SO}_4^{2-}) > \delta(\text{NH}_4^+) > \delta(\text{NO}_3^-)$,
410 SO_4^{2-} and NH_4^+ were sensitive to the NH_4^+ perturbation in the source profile, but NO_3^-
411 was not so sensitive.

412 In general, the simulation results of components in ambient $\text{PM}_{2.5}$ were affected in
413 one way or another by the change of source profiles adopted by CMAQ. Both of the
414 simulated Non-SNA and SNA were very sensitive to the perturbation of Non-SNA in
415 source profile. When the percentage of SNA changed in the source profile, simulated
416 concentrations of Non-SNA generally have little change, but the simulation results of
417 SNA could change in different levels: the simulated SO_4^{2-} was very sensitive and NH_4^+
418 was sensitive to the perturbation of SO_4^{2-} in source profile, simulated NO_3^- was very
419 sensitive and NH_4^+ was sensitive to the perturbation of NO_3^- , SO_4^{2-} and NH_4^+ were
420 sensitive to the perturbation of NH_4^+ . The simulated component such as SO_4^{2-} was
421 influenced not only by the change of SO_4^{2-} itself but also by other components like
422 some Non-SNA and NH_4^+ in the source profile. In other words, there was a linkage
423 effect, variation of some components in the source profile would bring changes to the



424 simulated results of other components.

425 **5 How the variation of source profile adopted in CTMs impact on the simulation**
426 **of chemical components in PM_{2.5}?**

427 The variation of species allocation in emission sources directly affected the
428 composition of aerosol system in CTMs. In CMAQv5.0.2, the aerosol thermodynamic
429 equilibrium process was carried out according to ISORROPIA II, including a SO₄²⁻-
430 NO₃⁻-Cl⁻-NH₄⁺-Na⁺-K⁺-Mg²⁺-Ca²⁺-H₂O system which was established on the basis of
431 ISORROPIA I by adding the effects of K⁺, Ca²⁺ and Mg²⁺ (Detailed equilibrium
432 relations were shown in Table S22). Some assumptions had been made in the
433 ISORROPIA model to simplify the simulation system (Fountoukis and Nenes, 2007):
434 (1) Because the vapor pressure of sulfuric acid and metal salts (such as Na⁺, Ca²⁺, K⁺,
435 Mg²⁺) were very low, it was assumed that all the sulfuric acid and metal salts in the
436 system existed in the aerosol phase; (2) For ammonia in the system, it was preferred to
437 have an irreversible reaction with sulfuric acid to produce ammonium sulfate. Only
438 when there was still surplus NH₃ after the neutralization of H₂SO₄, can it have a
439 reversible reaction with HNO₃ and HCl to produce NH₄NO₃ and NH₄Cl. (3) For sulfuric
440 acid in the system, if there were metal ions (such as Ca²⁺, Mg²⁺, K⁺, Na⁺) in the system,
441 sulfuric acid would react with metal ions to produce metal salts. Only in the case of
442 insufficient sodium, sulfuric acid would react with ammonia. Based on these
443 assumptions, the ISORROPIA model introduced the following three judgment
444 parameters (R₁, R₂ and R₃ were calculated by the following formulas) to determine the
445 simulation subsystems. In this paper, R₁, R₂, R₃ and the corresponding solid phase
446 species under different perturbation cases on source profiles were shown in Table 3.
447 These components achieved thermodynamic equilibrium in the order of preference for
448 more stable salts, obviously, the simulation processes of these components may
449 influence each other.

450
$$R_1 = \frac{[\text{NH}_4^+] + [\text{Ca}^{2+}] + [\text{K}^+] + [\text{Mg}^{2+}] + [\text{Na}^+]}{[\text{SO}_4^{2-}]} \dots\dots\dots (3)$$



451
$$R_2 = \frac{[Ca^{2+}] + [K^+] + [Mg^{2+}] + [Na^+]}{[SO_4^{2-}]} \dots\dots\dots (4)$$

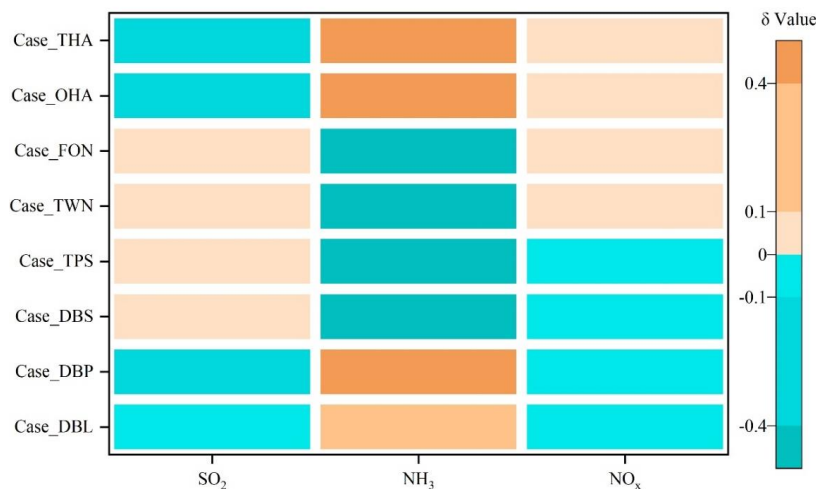
452
$$R_3 = \frac{[Ca^{2+}] + [K^+] + [Mg^{2+}]}{[SO_4^{2-}]} \dots\dots\dots (5)$$

453 Table 2 Potential aerosol species in ISORROPIA II under different cases

Cases	R ₁	R ₂	R ₃	Solid phase species*
SGL、DBL TWN、FON	2.53	2.52	1.9	CaSO ₄ , MgSO ₄ , K ₂ SO ₄ , Na ₂ SO ₄ , NaCl, NaNO ₃ , NH ₄ Cl, NH ₄ NO ₃
DBS	1.26	1.26	0.95	CaSO ₄ , MgSO ₄ , K ₂ SO ₄ , KHSO ₄ , Na ₂ SO ₄ , NaHSO ₄ , (NH ₄) ₂ SO ₄ , NH ₄ HSO ₄ , (NH ₄) ₃ H(SO ₄) ₂
TPS	0.84	0.84	0.63	CaSO ₄ , KHSO ₄ , NaHSO ₄ , NH ₄ HSO ₄
DBP	5.04	5.03	3.79	CaSO ₄ , MgSO ₄ , K ₂ SO ₄ , CaCl ₂ , Ca(NO ₃) ₂ , MgCl ₂ ,
OHA	3.58	2.52	2.95	Mg(NO ₃) ₂ , KCl, KNO ₃ , NaCl, NaNO ₃ , NH ₄ Cl,
THA	4.64	2.52	4.02	NH ₄ NO ₃

454 * The solid phase species were determined based on the research of (Fountoukis and Nenes, 2007)

455 In Non-SNA perturbation case, when the percentage of Non-SNA in source profile
 456 doubled (Case DBP), meant there were more Na, K, Mg, Ca, Cl participated in aerosol
 457 chemistry, the model system needed more SO₄²⁻ and NO₃⁻ on the basis of charge balance
 458 and the thermodynamic equilibrium shifted to the direction of consuming Ca Mg, K
 459 and Na, which resulted in the increase of the simulated concentration of SO₄²⁻ and NO₃⁻.
 460 Meanwhile, according to the rule of anions preferentially binding with nonvolatile
 461 cations in ISORROPIA, the increased cations Na⁺, K⁺, Mg²⁺, Ca²⁺ directly led to
 462 the decrease of anions binding with NH₄⁺, there were less reaction dose between SO₄²⁻
 463 and NH₄⁺ to form (NH₄)₂SO₄ or NH₄HSO₄, ultimately resulted in a decrease in
 464 simulated concentration of NH₄⁺ when compared to the base case. Because in this case
 465 more anions such as SO₄²⁻ were passively needed, according to the principle of chemical
 466 equilibrium mentioned above, the chemical conversion of SO₂ to SO₄²⁻ was promoted,
 467 the simulated secondary SO₄²⁻ increased, this could be proved by that the δ of SO₂ in
 468 Case DBP was negative (shown in Fig. 9, details of other monitoring stations were
 469 shown Table S24).



470
471 Fig.9 The sensitivity coefficients (δ) of simulated gas pollutants to the change of adopted source
472 profile in different cases.

473 Similarly, with the increase of metal ions in the system to bond with anions, the
474 number of anions which can bind to NH_4^+ decreased. The system needed less NH_4^+ and
475 weakened the need for conversion from NH_3 to NH_4^+ , the simulated NH_4^+ concentration
476 decreased while the δ of NH_3 was positive and very sensitive. Different trends of
477 simulated concentration of gaseous pollutants mirrored the rules mentioned above from
478 another aspect. The δ of SO_2 and NO_x was negative, NH_3 was positive. We could see
479 the same phenomena in DBL case (Fig. 9). When the percentages of Non-SNA in source
480 profile increased, they not only affected the simulated concentration of Non-SNA, but
481 also the secondary SO_4^{2-} , NO_3^- and NH_4^+ .

482 In SO_4^{2-} perturbation cases (Case DBS and TPS), as the percentage of SO_4^{2-} in
483 source profile increased, for the chemical reactions of sulfate radical consuming (as
484 shown in Table S22), the chemical equilibrium would move toward the products when
485 compared to the base case. While for the chemical reactions of sulfate radical formation
486 (The equations were shown in Table S23), meant the product was added in, the chemical
487 equilibrium would be pushed toward the reactants. The chemical reactions between
488 SO_4^{2-} and NH_4^+ would shift to the direction of $(\text{NH}_4)_2\text{SO}_4$ generation, we could see the
489 simulated concentrations of NH_4^+ in DBS and TPS were both higher and NH_3 were
490 lower than those in the base case (SGL). In addition, when more SO_4^{2-} was added in,



491 the conversion of SO_2 to SO_4^{2-} was affected in some level and consumed less SO_2 than
492 the base case, simulated SO_2 showed insensitive but positive trend (Fig.9). And from
493 the potential solid phase species in ISORROPIA II under DBS and TPS cases (Table 3),
494 the solid phase species were mainly consisted of sulfate salts, so the simulated
495 concentration of NO_3^- did not change apparently.

496 As the percentage of NO_3^- in source profile increased (Case FON and TWN), the
497 associated chemical equilibrium shifted towards the consumption of NO_3^- , such as NH_4^+
498 + $\text{NO}_3^- \rightarrow \text{NH}_4\text{NO}_3$, which would also consume more NH_4^+ and form more ammonium
499 salt, finally consumed more NH_3 because of $\text{NH}_3(\text{gas}) + \text{H}_2\text{O}(\text{aq}) \rightarrow \text{NH}_4^+(\text{aq}) + \text{OH}^-$
500 (aq). The simulation results also manifested that the concentration of NH_4^+ increased
501 while that of NH_3 decreased. Based on the assumption of ISORROPIA, the cations like
502 Na^+ , K^+ , Mg^{2+} , Ca^{2+} and NH_4^+ preferentially to react with SO_4^{2-} , only if there were
503 cations left after neutralized SO_4^{2-} , could they react with NO_3^- to form salts, so the
504 simulated concentration of SO_4^{2-} was not obviously changed. Accordingly, the
505 simulated concentration of NO_x and SO_2 almost unchanged (The δ of NO_x and SO_2 was
506 insensitive).

507 In the cases of NH_4^+ perturbation (Case OHA and THA), when the percentage of
508 NH_4^+ in source profile increased, the related chemical equilibrium shifted towards the
509 direction of NH_4^+ consumption, such as in $2\text{NH}_4^+ + \text{SO}_4^{2-} \rightarrow (\text{NH}_4)_2\text{SO}_4$, more SO_4^{2-}
510 was consumed at the same time, which further promoted the conversion of SO_2 to SO_4^{2-} .
511 The increased NH_4^+ in OHA and THA also would inhibit the conversion of NH_3 to NH_4^+
512 when compared to the base case. This, in turn appeared as the increase of the simulated
513 secondary SO_4^{2-} and NH_3 , and the decrease of the simulated SO_2 .

514 In summary, the effects of source profile variation on the simulation results of
515 different components were linked. When the percentages of Non-SNA, SO_4^{2-} , NO_3^- and
516 NH_4^+ in the source profile changed, they not only affected the simulated concentration
517 of themselves, but also affected the simulation results of some other components. Both
518 the simulation results of primary components and secondary components were affected
519 by the change of source profile, the secondary SO_4^{2-} and NH_4^+ were affected more than



520 the secondary NO_3^- .

521 **6 Conclusions**

522 Although the influence of source profile variation on the simulated concentration
523 of ambient $\text{PM}_{2.5}$ is not significant, its influence on the simulated chemical components
524 cannot be ignored. The variation of simulated components ranges from 8% to 167%
525 under selected different source profiles, and the simulation results of some components
526 are sensitive to the adopted $\text{PM}_{2.5}$ source profile in CTMs, e.g., both the simulated Non-
527 SNA and SNA are sensitive to the perturbation of Non-SNA in source profile, the
528 simulated SO_4^{2-} and NH_4^+ are sensitive to the perturbation of SO_4^{2-} , simulated NO_3^- and
529 NH_4^+ are sensitive to the perturbation of NO_3^- , SO_4^{2-} and NH_4^+ are sensitive to the
530 perturbation of NH_4^+ . These influences are not only specific to an individual component,
531 but also can be transmitted and linked among components, that is, the influence path is
532 connected to chemical mechanisms in the model since the variation of species allocation
533 in emission sources directly affect the thermodynamic equilibrium system
534 (ISORROPIA II, SO_4^{2-} - NO_3^- - Cl^- - NH_4^+ - Na^+ - K^+ - Mg^{2+} - Ca^{2+} - H_2O system).

535 Traditionally, the source profiles are regarded as a primary emission, but
536 interestingly, their variation could affect the simulation result of secondary components
537 as well in CTMs. We found the perturbation of $\text{PM}_{2.5}$ source profile caused the variation
538 of simulated gaseous pollutants, and related chemical reactions like gas-phase
539 chemistry of SO_2 , NO_x and NH_3 , which mirrored that the perturbation of source profile
540 had an effect on the simulation of secondary $\text{PM}_{2.5}$ components. Overall, the emission
541 source profile used in CTMs is one of the important factors affecting the simulation
542 results of $\text{PM}_{2.5}$ chemical components. Additionally, organic species are one of the most
543 important components in $\text{PM}_{2.5}$ and gain much more attention on human health. While
544 the number of organic species in source profile is relatively scarce which brings a
545 challenge for simulation test designing, the variation of source profile adopted in CTMs
546 has an impact on the simulation of organic species is not taken into account in this study.

547 With the change of fuel and raw materials, the development of production



548 technology and the innovation of pollution treatment technology in recent years, some
549 components have changed significantly in the source profile. Given the important role
550 of air quality simulation in environment management and health risk assessment, the
551 representativeness and timeliness of the source profile should be considered.

552 **Data availability**

553 The input datasets for WRF simulation are available at
554 <https://rda.ucar.edu/datasets/ds351.0/index.html> (The National Center for Atmospheric
555 Research (NCAR)). The Multi-resolution Emission Inventory for China (MEICv1.3) is
556 available at http://meicmodel.org/?page_id=135. The PM_{2.5} emission source profiles
557 from database of Source Profiles of Air Pollution (SPAP)
558 (<http://www.nkspap.com:9091/>, Nankai university), SPECIATE database
559 (<https://www.epa.gov/air-emissions-modeling/speciate>, U.S. Environmental Protection
560 Agency's (EPA)), Mendeley data repository (<https://doi.org/10.17632/x8dfshjt9j.2>, Bi
561 et al., 2019).

562 **Code availability**

563 The source code for CMAQ version 5.0.2 is available at
564 <https://github.com/USEPA/CMAQ/tree/5.0.2> (last access: April 2014)
565 (<https://doi.org/10.5281/zenodo.1079898>, US EPA Office of Research and
566 Development, 2018). The source code for WRF version 3.7.1 is available at
567 <https://github.com/NCAR/WRFV3> (last access: 14 August 2015, NCAR).

568 **Author contributions**

569 Zhongwei Luo: Data curation and collection, writing—original draft. Yan Han:
570 Modeling, writing—original draft. Kun Hua: Data collection. Yufen Zhang:
571 Supervision—Review & editing. Jianhui Wu: Supervision in source profile. Xiaohui Bi:
572 Supervision in source profile. Qili Dai: Resources. Baoshuang Liu: Resources. Yang
573 Chen: Modification and editing. Xin Long: Supervision in modeling. Yinchang Feng:
574 Supervision—Review & editing.



575 **Competing interests**

576 The authors declare that they have no known competing financial interests or
577 personal relationships that could have appeared to influence the work reported in this
578 paper.

579 **Disclaimer. Publisher's note**

580 Copernicus Publications remains neutral with regard to jurisdictional claims in
581 published maps and institutional affiliations.

582 **Acknowledgements**

583 We would like to thank the National Natural Science Foundation of China (grant
584 number 42177465) for providing funding for the project. We are grateful for the
585 Inventory Spatial Allocate Tool (ISAT) provided by Kun Wang from Department of Air
586 Pollution Control, Institute of Urban Safety and Environmental Science, Beijing
587 Academy of Science and Technology.

588 **Financial support**

589 This study was financially supported by the National Natural Science Foundation
590 of China (grant number 42177465).

591 **Reference**

- 592 Appel, K. W., Poullo, G. A., Simon, H., Sarwar, G., Pye, H. O. T., Napelenok, S. L., Akhtar, F., Roselle,
593 S. J.: Evaluation of dust and trace metal estimates from the Community Multiscale Air Quality
594 (CMAQ) model version 5.0, *Geosci. Model Dev.*, 6, 883-899, [https://doi.org/10.5194/gmd-6-883-](https://doi.org/10.5194/gmd-6-883-2013)
595 2013, 2013.
- 596 Bi, X., Dai, Q., Wu, J., Zhang, Q., Zhang, W., Luo, R., Cheng, Y., Zhang, J., Wang, L., Yu, Z., Zhang, Y.,
597 Tian, Y., Feng, Y.: Characteristics of the main primary source profiles of particulate matter across
598 China from 1987 to 2017, *Atmos. Chem. Phys.*, 19, 3223-3243, [https://doi.org/10.5194/acp-19-](https://doi.org/10.5194/acp-19-3223-2019)
599 3223-2019, 2019.
- 600 Cao, J., Qiu, X., Gao, J., Wang, F., Wang, J., Wu, J., Peng, L.: Significant decrease in SO₂ emission and
601 enhanced atmospheric oxidation trigger changes in sulfate formation pathways in China during
602 2008–2016, *J. Clean. Prod.*, 326, 129396, <https://doi.org/10.1016/j.jclepro.2021.129396>, 2021.
- 603 Chapel Hill, N.: Operational Guidance for the Community Multiscale Air Quality (CMAQ) Mo
604 deling System Version 5.0, https://www.airqualitymodeling.org/index.php/CMAQ_version_5.0
605 (February_2010_release)_OGD#Aerosol_Module, last access: February 2012.



- 606 Chen, Z., Chen, D., Zhao, C., Kwan, M., Cai, J., Zhuang, Y., Zhao, B., Wang, X., Chen, B., Yang, J., Li,
607 R., He, B., Gao, B., Wang, K., Xu, B.: Influence of meteorological conditions on PM_{2.5}
608 concentrations across China: A review of methodology and mechanism, *Environ. Int.*, 139, 105558,
609 <https://doi.org/10.1016/j.envint.2020.105558>, 2020.
- 610 Cheng, N. L., Meng, F., Wang, J. K., Chen, Y. B., Wei, X., Han, H.: Numerical simulation of the spatial
611 distribution and deposition of PM_{2.5} in East China coastal area in 2010 (In Chinese), *Journ. Safety
612 Environ.*, 15, 305-310, <https://doi.org/10.13637/j.issn.1009-6094.2015.06.063>, 2015.
- 613 Foley, K. M., Roselle, S. J., Appel, K. W., Bhawe, P. V., Pleim, J., Otte, T., Mathur, R., Sarwar, G., Young,
614 J. O., Gilliam, R.: Incremental testing of the community multiscale air quality (CMAQ) modeling
615 system version 4.7, *Geosci. Model Dev.*, 3, 205-226, <https://doi.org/10.5194/gmd-3-205-2010>, 2010.
- 616 Fountoukis, C., Nenes, A.: ISORROPIA II: a computationally efficient thermodynamic equilibrium
617 model for K⁺-Ca²⁺-Mg²⁺-NH₄⁺-Na⁺-SO₄²⁻-NO₃⁻-Cl⁻-H₂O aerosols, *Atmos. Chem. Phys.*, 7,
618 4639-4659, <https://doi.org/10.5194/acp-7-4639-2007>, 2007.
- 619 Fu, X., Wang, S., Zhao, B., Xing, J., Cheng, Z., Liu, H., Hao, J.: Emission inventory of primary pollutants
620 and chemical speciation in 2010 for the Yangtze River Delta region, China, *Atmos. Environ.*, 70,
621 39-50, <https://doi.org/10.1016/j.atmosenv.2012.12.034>, 2013.
- 622 Fu, X., Wang, S. X., Chang, X., Cai, S., Xing, J., Hao, J. M.: Modeling analysis of secondary inorganic
623 aerosols over China: pollution characteristics, and meteorological and dust impacts, *Sci. Rep.*, 6,
624 35992, <https://doi.org/10.1038/srep35992>, 2016.
- 625 Gao, S., Zhang, S., Che, X., Ma, Y., Chen, X., Duan, Y., Fu, Q., Wang, S., Zhou, B., Wei, C., Jiao, Z.:
626 New understanding of source profiles: Example of the coating industry, *J. Clean. Prod.*, 357, 132025,
627 <https://doi.org/10.1016/j.jclepro.2022.132025>, 2022.
- 628 Guo, R., Yang, J., Liu, Z.: Influence of heat treatment conditions on release of chlorine from Datong coal,
629 *J. Anal. Appl. Pyrol.*, 71, 179-186, [https://doi.org/10.1016/S0165-2370\(03\)00086-X](https://doi.org/10.1016/S0165-2370(03)00086-X), 2004.
- 630 Guo, Y. Y., Gao, X., Zhu, T. Y., Luo, L., Zheng, Y.: Chemical profiles of PM emitted from the iron and
631 steel industry in northern China, *Atmos. Environ.*, 150, 187-197,
632 <https://doi.org/10.1016/j.atmosenv.2016.11.055>, 2017.
- 633 Guo, Z., Hao, Y., Tian, H., Bai, X., Wu, B., Liu, S., Luo, L., Liu, W., Zhao, S., Lin, S., Lv, Y., Yang, J.,
634 Xiao, Y.: Field measurements on emission characteristics, chemical profiles, and emission factors
635 of size-segregated PM from cement plants in China, *Sci. Total Environ.*, 151822,
636 <https://doi.org/10.1016/j.scitotenv.2021.151822>, 2021.
- 637 Han, Y., Xu, H., Bi, X. H., Lin, F. M., Li, J., Zhang, Y. F., Feng, Y. C.: The effect of atmospheric
638 particulates on the rainwater chemistry in the Yangtze River Delta, China, *J. Air Waste Manage.*, 69,
639 1452-1466, <https://doi.org/10.1080/10962247.2019.1674750>, 2019.
- 640 Hopke, P. K., Dai, Q., Li, L., Feng, Y.: Global review of recent source apportionments for airborne
641 particulate matter, *Sci. Total Environ.*, 740, 140091,
642 <https://doi.org/10.1016/j.scitotenv.2020.140091>, 2020.
- 643 Hopke, P. K., Feng, Y. C., Dai, Q.: Source apportionment of particle number concentrations: A global
644 review, *Sci. Total Environ.*, 819, 153104, <https://doi.org/10.1016/j.scitotenv.2022.153104>, 2022.
- 645 Hsu, Y., Divita, F., Dorn, J.: SPECIATE 5.0 - Speciation Database Development Documentation, Final
646 Report, M. MENETREZ, Abt Associates Inc./Office of Research and Development/U.S.
647 Environmental Protection Agency Research Triangle Park, NC27711,
648 https://www.epa.gov/sites/default/files/2019-07/documents/speciate_5.0.pdf, 2019.
- 649 Huang, C. H., Hu, J. L., Xue, T., Xu, H., Wang, M.: High-Resolution Spatiotemporal Modeling for



- 650 Ambient PM_{2.5} Exposure Assessment in China from 2013 to 2019, *Environ. Sci. Technol.*, 55, 2152-
651 2162, <https://doi.org/10.1021/acs.est.0c05815>, 2021.
- 652 Huang, Z. J., Zheng, J. Y., Qu, J. M., Zhong, Z. M., Wu, Y. Q., Shao, M.: A Feasible Methodological
653 Framework for Uncertainty Analysis and Diagnosis of Atmospheric Chemical Transport Models,
654 *Environ. Sci. Technol.*, 53, 3110-3118, <https://doi.org/10.1021/acs.est.8b06326>, 2019.
- 655 Ji, Z., Gan, M., Fan, X., Chen, X., Li, Q., Lv, W., Tian, Y., Zhou, Y., Jiang, T.: Characteristics of PM_{2.5}
656 from iron ore sintering process: Influences of raw materials and controlling methods, *J. Clean. Prod.*,
657 148, 12-22, <https://doi.org/10.1016/j.jclepro.2017.01.103>, 2017.
- 658 Li, J., Wu, Y., Ren, L., Wang, W., Tao, J., Gao, Y., Li, G., Yang, X., Han, Z., Zhang, R.: Variation in PM_{2.5}
659 sources in central North China Plain during 2017–2019: Response to mitigation strategies, *J.*
660 *Environ. Manage.*, 28, 112370, <https://doi.org/10.1016/j.jenvman.2021.112370>, 2021.
- 661 Li, M., Hu, M., Du, B., Guo, Q., Tan, T., Zheng, J., Huang, X., He, L., Wu, Z., Guo, S.: Temporal and
662 spatial distribution of PM_{2.5} chemical composition in a coastal city of Southeast China, *Sci. Total*
663 *Environ.*, 605-606, 337-346, <https://doi.org/10.1016/j.scitotenv.2017.03.260>, 2017a.
- 664 Li, M., Liu, H., Geng, G., Hong, C., Liu, F., Song, Y., Tong, D., Zheng, B., Cui, H., Man, H., Zhang, Q.,
665 He, K.: Anthropogenic emission inventories in China: a review, *Natl. Sci. Rev.*, 4, 834-866,
666 <https://doi.org/10.1093/nsr/nwy044>, 2017b.
- 667 Li, X., He, K., Li, C., Yang, F., Zhao, Q., Ma, Y., Chen, Y., Ouyang, W., Chen, G.: PM_{2.5} mass, chemical
668 composition, and light extinction before and during the 2008 Beijing Olympics, *J. Geophys. Res.*,
669 118, 12158-12167, <https://doi.org/10.1002/2013JD020106>, 2013.
- 670 Liang, F., Xiao, Q., Yang, X., Liu, F., Li, J., Lu, X., Liu, Y., Gu, D.: The 17-y spatiotemporal trend of
671 PM_{2.5} and its mortality burden in China, *Proc. Natl. Acad. Sci.*, 117, 25601-25608,
672 <https://doi.org/10.1073/pnas.1919641117>, 2020.
- 673 Lv, L., Wei, P., Li, J., Hu, J.: Application of machine learning algorithms to improve numerical simulation
674 prediction of PM_{2.5} and chemical components, *Atmos. Pollut. Res.*, 12, 101211,
675 <https://doi.org/10.1016/j.apr.2021.101211>, 2021.
- 676 NBS (National Bureau of Statistics of China): China Statistical Yearbook 2021,
677 <http://www.stats.gov.cn/tjsj/ndsj/2021/indexch.htm>, last access: 2022.
- 678 Peterson, G., Hogrefe, C., Corrigan, A., Neas, L., Mathur, R., Rappold, A.: Impact of Reductions in
679 Emissions from Major Source Sectors on Fine Particulate Matter–Related Cardiovascular Mortality,
680 *Environ. Health Persp.*, 128, 017005, <https://doi.org/10.1289/EHP5692>, 2020.
- 681 Qi, H., Cui, C., Zhao, T., Bai, Y., Liu, L.: Numerical simulation on the characteristics of PM_{2.5} heavy
682 pollution and the influence of weather system in Hubei Province in winter 2015 (In Chinese),
683 *Meteorological monthly*, 45, 1113-1122, <https://doi.org/10.7519/j.issn.1000-0526.2019.08.008>,
684 2019.
- 685 Seinfeld, J. H., Pandis, S. N.: Atmospheric Chemistry and Physics, from air pollution to climate change.
686 John Wiley & Sons, Inc., Hoboken, New Jersey.47-61, ISBN9781119221166, 2006
- 687 Sha, T., Ma, X., Jia, H., Tian, R., Chang, Y., Cao, F., Zhang, Y.: Aerosol chemical component: Simulations
688 with WRF-Chem and comparison with observations in Nanjing, *Atmos. Environ.*, 218, 1-14,
689 <https://doi.org/10.1016/j.atmosenv.2019.116982>, 2019.
- 690 Shi, W., Liu, C., Norback, D., Deng, Q., Huang, C., Qian, H., Zhang, X., Sundell, J., Zhang, Y., Li, B.,
691 Kan, H., Zhao, Z.: Effects of fine particulate matter and its constituents on childhood pneumonia: a
692 cross-sectional study in six Chinese cities, *Lancet*, 392, S79, [https://doi.org/10.1016/S0140-6736\(18\)32708-9](https://doi.org/10.1016/S0140-6736(18)32708-9), 2018.



- 694 Shi, Z., Li, J., Huang, L., Wang, P., Wu, L., Ying, Q., Zhang, H., Lu, L., Liu, X., Liao, H., Hu, J.: Source
695 apportionment of fine particulate matter in China in 2013 using a source-oriented chemical transport
696 model, *Sci. Total Environ.*, 601-602, 1476-1487, <https://doi.org/10.1016/j.scitotenv.2017.06.019>,
697 2017.
- 698 Song, S. Y., Wang, Y. S., Wang, Y. L., Wang, T., Tan, H. Z.: The characteristics of particulate matter and
699 optical properties of Brown carbon in air lean condition related to residential coal combustion,
700 *Powder Technol.*, 379, 505-514, <https://doi.org/10.1016/j.powtec.2020.10.082>, 2021.
- 701 Tang, X. Y., Zhang, Y. H., Shao, M.: *Atmosphere Environment Chemistry, Second ed (In Chinese)*. .
702 Higher Education Press, Beijing, China.268-329, ISBN978-7-04-019361-9, 2006
- 703 Wang, C., Zheng, J., Du, J., Wang, G., Klemes, J., Wang, B., Liao, Q., Liang, Y.: Weather condition-
704 based hybrid models for multiple air pollutants forecasting and minimisation, *J. Clean. Prod.*, 352,
705 131610, <https://doi.org/10.1016/j.jclepro.2022.131610>, 2022.
- 706 Wang, D., Hu, J., Xu, Y., Lv, D., Xie, X., Kleeman, M., Xing, J., Zhang, H., Ying, Q.: Source
707 contributions to primary and secondary inorganic particulate matter during a severe wintertime
708 PM_{2.5} pollution episode in Xi'an, China, *Atmos. Environ.*, 97, 182-194,
709 <https://doi.org/10.1016/j.atmosenv.2014.08.020>, 2014.
- 710 Weagle, C., Sinder, G., Li, C. C., Donkelaar, A., S, P., Bissonnette, P., Burke, I., Jackson, J., Latimer, R.,
711 Stone, E., Abboud, I., Akoshile, C., Anh, N., Brook, J., Cohen, A., Dong, J., Gibson, M., Griffith,
712 D., He, K., Holben, B., Kahn, R., Keller, C., Kim, J., Lagrosas, N., Lestari, P., Khian, Y., Liu, Y.,
713 Marais, E., Martins, J., Misra, A., Muliane, U., Pratiwi, R., Quel, E., Salam, A., Segey, L., Tripathi,
714 S., Wang, C., Zhang, Q., Brauer, M., Rudich, Y., Martin, R.: Global Sources of Fine Particulate
715 Matter: Interpretation of PM_{2.5} Chemical Composition Observed by SPARTAN using a Global
716 Chemical Transport Model, *Environ. Sci. Technol.*, 52, 11670-11681,
717 <https://doi.org/10.1021/acs.est.8b01658>, 2018.
- 718 Wongphatarakul, V., Friedlander, S. K., Pinto, J. P.: A Comparative Study of PM_{2.5} Ambient Aerosol
719 Chemical Databases, *Environ. Sci. Technol.*, 32, 3926-3934, <https://doi.org/10.1021/es9800582>,
720 1998.
- 721 Wu, B., Bai, X., Liu, W., Zhu, C., Hao, Y., Lin, S., Liu, S., Luo, L., Liu, X., Zhao, S., Hao, J., Tian, H.:
722 Variation characteristics of final size-segregated PM emissions from ultralow emission coal-fired
723 power plants in China, *Environ. Pollut.*, 259, 113886, <https://doi.org/10.1016/j.envpol.2019.113886>,
724 2020.
- 725 Wu, D., Zheng, H., Li, Q., Jin, L., Lyu, R., Ding, X., Huo, Y., Zhao, B., Jiang, J., Chen, J., Li, X., Wang,
726 S.: Toxic potency-adjusted control of air pollution for solid fuel combustion, *Nat. Energy*, 7, 194-
727 202, <https://doi.org/10.1038/s41560-021-00951-1>, 2022.
- 728 Wu, Z. X., Hu, T. F., Hu, W., Shao, L. Y., Sun, Y. Z., Xue, F. L., Niu, H. Y.: Evolution in physicochemical
729 properties of fine particles emitted from residential coal combustion based on chamber experiment,
730 *Gondwana Res.*, <https://doi.org/10.1016/j.gr.2021.10.017>, 2021.
- 731 Xia, Z. Q., Fan, X. L., Huang, Z. J., Liu, Y. C., Yin, X. H., Ye, X., Zheng, J. Y.: Comparison of Domestic
732 and Foreign PM_{2.5} Source Profiles and Influence on Air Quality Simulation (In Chinese), *Res.*
733 *Environ. Sci.*, 30, 359-367, <https://doi.org/10.13198/j.issn.1001-6929.2017.01.55>, 2017.
- 734 Yang, F., Tan, J., Zhao, Q., Du, Z., He, K., Ma, Y., Duan, F., Chen, G., Zhao, Q.: Characteristics of PM_{2.5}
735 speciation in representative megacities and across China, *Atmos. Chem. Phys.*, 11, 1025-1051,
736 <https://doi.org/10.5194/acpd-11-1025-2011>, 2011.
- 737 Ying, Q., Feng, M., Song, D. L., Wu, L., Hu, J., Zhang, H., Kleeman, M., Li, X.: Improve regional



738 distribution and source apportionment of PM_{2.5} trace elements in China using inventory-observation
739 constrained emission factors, *Sci. Total Environ.*, 624, 355-365,
740 <https://doi.org/10.1016/j.scitotenv.2017.12.138>, 2018.

741 Yu, Z. C., Jang, M., Kim, S., Bae, C., Koo, B., Beardsley, R., Park, J., Chang, L., Lee, H., Lim, Y., Cho,
742 J.: Simulating the Impact of Long-Range-Transported Asian Mineral Dust on the Formation of
743 Sulfate and Nitrate during the KORUS-AQ Campaign, *Earth Space Chem.*, 4, 1039-1049,
744 <https://doi.org/10.1021/acsearthspacechem.0c00074>, 2020.

745 Zhang, J., Wu, J., Lv, R., Song, D., Huang, F., Zhang, Y., Feng, Y.: Influence of Typical Desulfurization
746 Process on Flue Gas Particulate Matter of Coal-fired Boilers (In Chinese), *Environ. Sci.*, 41, 4455-
747 4461, <https://doi.org/10.13227/j.hjcx.202003193>, 2020.

748 Zhang, Q., Xue, D., Wang, S., Wang, L., Wang, J., Ma, Y., Liu, X.: Analysis on the evolution of PM_{2.5}
749 heavy air pollution process in Qingdao (In Chinese), *China Environ. Sci.*, 37, 3623-3635,
750 <https://doi.org/10.3969/j.issn.1000-6923.2017.10.003>, 2017.

751 Zhang, S. P., Xing, J., Sarwar, G., Ge, Y. L., He, H., Duan, F., Zhao, Y., He, K., Zhu, L., Chu, B.:
752 Parameterization of heterogeneous reaction of SO₂ to sulfate on dust with coexistence of NH₃ and
753 NO₂ under different humidity conditions, *Atmos. Environ.*, 208, 133-140,
754 <https://doi.org/10.1016/j.atmosenv.2019.04.004>, 2019.

755 Zheng, B., Tong, D., Li, M., Liu, F., Hong, C., Geng, G., Li, H., Li, X., Peng, L., Qi, J., Yan, L., Zhang,
756 Y., Zhao, H., Zheng, Y., He, K., Zhang, Q.: Trends in China's anthropogenic emissions since 2010
757 as the consequence of clean air actions, *Atmos. Chem. Phys.*, 18, 14095-14111,
758 <https://doi.org/10.5194/acp-18-14095-2018>, 2018.

759 Zheng, B., Zhang, Q., Zhang, Y., He, K. B., Wang, K., Zheng, G. J., Duan, F. K., Ma, Y. L., Kimoto, T.:
760 Heterogeneous chemistry: a mechanism missing in current models to explain secondary inorganic
761 aerosol formation during the January 2013 haze episode in North China, *Atmos. Chem. Phys.*, 15,
762 2031–2049, <https://doi.org/10.5194/acp-15-2031-2015>, 2015.

763 Zheng, H., Song, S., Sarwar, G., Gen, M., Wang, S., Ding, D., Chang, X., Zhang, S., Xing, J., Sun, Y. L.,
764 Ji, D., Chan, C. K., Gao, J., McElroy, M.: Contribution of Particulate Nitrate Photolysis to
765 Heterogeneous Sulfate Formation for Winter Haze in China, *Environ. Sci. Technol. Lett.*, 7, 632-
766 638, <https://doi.org/10.1021/acs.estlett.0c00368>, 2020.

767 Zhou, L., Chen, X., Tian, X.: The impact of fine particulate matter (PM_{2.5}) on China's agricultural
768 production from 2001 to 2010, *J. Clean. Prod.*, 178, 133-141,
769 <https://doi.org/10.1016/j.jclepro.2017.12.204>, 2018.

770